Original Article

MOLECULAR METABOLISM

Long-chain acyl-CoA synthetase-4 regulates endometrial decidualization through a fatty acid β-oxidation pathway rather than lipid droplet accumulation

Hongshuo Zhang[1,2,3], Qianyi Sun[1,3], Haojie Dong[1,3], Zeen Jin[1], Mengyue Li[1], Shanyuan Jin[1], Xiaolan Zeng[1], Jianhui Fan[1,], Ying Kong[1,*]**

ABSTRACT

Objective: Lipid metabolism plays an important role in early pregnancy, but its effects on decidualization are poorly understood. Fatty acids (FAs) must be esterified by fatty acyl-CoA synthetases to form biologically active acyl-CoA in order to enter the anabolic and/or catabolic pathway. Long-chain acyl-CoA synthetase 4 (ACSL4) is associated with female reproduction. However, whether it is involved in decidualization is unknown.
Methods: The expression of ACSL4 in human and mouse endometrium was detected by immunohistochemistry. ACSL4 levels were regulated by the overexpression of ACSL4 plasmid or ACSL4 siRNA, and the effects of ACSL4 on decidualization markers and morphology of endometrial stromal cells (ESCs) were clarified. A pregnant mouse model was established to determine the effect of ACSL4 on the implantation efficiency of mouse embryos. Modulation of ACSL4 detects lipid anabolism and catabolism.
Results: Through examining the expression level of ACSL4 in human endometrial tissues during proliferative and secretory phases, we found that ACSL4 was highly expressed during the secretory phase. Knockdown of ACSL4 suppressed decidualization and inhibited the mesenchymal-to-epithelial transition induced by MPA and db-cAMP in ESCs. Further, the knockdown of ACSL4 reduced the efficiency of embryo implantation in pregnant mice. Downregulation of ACSL4 inhibited FA β-oxidation and lipid droplet accumulation during decidualization. Interestingly, pharmacological and genetic inhibition of lipid droplet synthesis did not affect FA β-oxidation and decidualization, while the pharmacological and genetic inhibition of FA β-oxidation increased lipid droplet accumulation and inhibited decidualization. In addition, inhibition of β-oxidation was found to attenuate the promotion of decidualization by the upregulation of ACSL4. The decidualization damage caused by ACSL4 knockdown could be reversed by activating β-oxidation.
Conclusions: Our findings suggest that ACSL4 promotes endometrial decidualization by activating the β-oxidation pathway. This study provides interesting insights into our understanding of the mechanisms regulating lipid metabolism during decidualization.

Keywords ACSL4; Endometrium; Decidualization; Lipid metabolism; Fatty acid β-oxidation; Lipid droplet

1. INTRODUCTION

Successful implantation of embryos requires synchronous development between the embryo and endometrium. The embryo has long been the focus of attention in reproductive studies. However, it is currently believed that the abnormal initiation (decidualization) of the endometrium may be more likely to cause reproductive disorders than the quality of the embryo [1]. The endometrium is a highly dynamic tissue with the ability to undergo a variety of physiological changes, including structural, molecular, and cellular changes, in response to estrogen and progesterone [2]. The main function of the endometrium is to enter a receptive state during the implantation window period [3], and the functional and morphological changes required are called decidualization. Decidualization allows the endometrium to form a decidual lining for blastocyst implantation and mainly includes endometrial stromal cells (ESCs) that begin to proliferate and differentiate into large, round, cytoplasmic-rich epithelioid cells (decidual cells). Healthy decidua is an important foundation for subsequent pregnancy,

[1]Department of Biochemistry and Molecular Biology, College of Basic Medical Sciences, Dalian Medical University, Dalian, China [2]Advanced Institute for Medical Sciences, Dalian Medical University, Dalian, China

[3] These authors contributed equally to this work.

*Corresponding author. Department of Biochemistry and Molecular Biology, College of Basic Medical Sciences, Dalian Medical University, Dalian, 116044, Liaoning, China. E-mail: yingkong@dmu.edu.cn (Y. Kong).

**Corresponding author. Department of Biochemistry and Molecular Biology, College of Basic Medical Sciences, Dalian Medical University, Dalian, 116044, Liaoning, China. E-mail: ephin@126.com (J. Fan).

Received February 29, 2024 • Revision received April 25, 2024 • Accepted April 29, 2024 • Available online 4 May 2024

https://doi.org/10.1016/j.molmet.2024.101953

Abbreviations

AA	arachidonic acid
ACS	acyl-CoA synthetase
ACSL	Long-chain acyl-CoA synthetase
ACSL4	Long-chain acyl-CoA synthetase-4
CPT	carnitine palmitoyl transferase
db-cAMP	dibutyryl-cAMP (dibutyryl-cyclic adenosine monophosphate)
DAG	diacylglycerol
DGAT2	diacylglycerol acyltransferase 2
ESCs	endometrial stromal cells
$FADH_2$	flavin adenine dinucleotide
FAs	Fatty acids
FOX01	forkhead box 01
GPAT4	glycerol-sn-3-phosphate acyltransferase 4
HOXA10	homeobox A10
IGFBP1	insulin-like growth factor-binding protein 1
iTRAQ	isobaric tags for relative and absolute quantification
LDs	lipid droplets
MPA	medroxyprogesterone acetate
NADH	nicotinamide adenine dinucleotide
PI3K	phosphatidylinositol 3-kinase
PKB/AKT	protein kinase B
PRL	prolactin
PUFAs	polyunsaturated fatty acids
TAG	triacylglycerol
TCA	tricarboxylic acid

and an abnormal decidua may lead to pregnancy failure or related pregnancy diseases.

Lipid metabolism plays an important role in early pregnancy, but the exact mechanism by which it regulates successful implantation remains unclear [4,5]. Growing evidence appears, which suggests lipid metabolism and fat mobilization have a profound impact on embryo quality and the uterine microenvironment [6]. Despite the achievements of scientists in improving embryo quality and selection, progress in understanding how lipid metabolism affects endometrial function lags behind blastocyst biology [7,8]. Recent studies have shown that the levels of total ω-6 polyunsaturated fatty acids (PUFAs), arachidonic acid (AA), and linoleic acid in mouse uterine tissues positively correlated with the embryo implantation rate [9]. In this regard, a disorder of lipid metabolism may reduce the implantation ability of the endometrium [8]. In addition, the regulation of lipid metabolic profiles during pregnancy may serve as a compensatory strategy for energy expenditure [5]. Therefore, it is of great significance to understand the role of lipid metabolism in endometrial decidualization.

Fatty acids are the main energy source of mammals. In the process of lipid metabolism, both exogenous and endogenous FAs must be esterified to form bioactive fatty acyl-CoA through acyl-CoA synthetase (ACS) to enter the relevant metabolic pathways. This includes FA oxidation mediated by an intracellular β-oxidation system as well as the synthesis of triacylglycerol (TAG), phospholipids, and cholesterol esters. Studies have shown that the accumulation of free FAs in the endometrium and lipotoxicity may prevent ESCs from proper decidualization [10]. Reports claimed that the accumulation of lipid droplets (LDs) in ESCs increased during decidualization [11]. Long-chain acyl-CoA synthetase (ACSL) catalyzes the activation of a large number of FAs, ranging from 12 to 22 carbon chain lengths [12], and thus plays a key role in lipid metabolism. Five subtypes of ACSLs exist: ACSL1, ACSL3, ACSL4, ACSL5, and ACSL6 [13]. Several differences exist in the tissue distribution of the subtypes: ACSL1 is generally distributed in the liver and myocardial tissue [14]. ACSL3 and ACSL6 are mostly found in the brain and skeletal muscle [15]. ACSL5 is highly expressed in the intestinal mucosa and plays an important role in the absorption of food-derived lipids [16]. ACSL4 is mainly expressed in steroid-synthesizing tissues such as the adrenal gland, ovary, placenta, and testis [17], and is associated with steroid hormone and growth factor receptors [18]. Recent studies have shown that ACSL4 is upregulated in cancers originating from tissues with high levels of basal lipid metabolism, such as liver and colon cancers [19,20]. ACSL4 regulates de novo adipose synthesis by accumulating intracellular TAG, cholesterol, and lipid droplets in hepatocellular carcinoma [21], and participates in processes such as female fertility [22]. However, whether ACSL4 is involved in the decidual process in the endometrium has not been reported as yet.

In this study, we investigated the expression of ACSL4 during the implantation window of the endometrium. We found that the regulation of ACSL4 can affect decidualization as well as lipid accumulation and β-oxidation levels in decidual cells. Further, we found that ACSL4 regulates ESC decidualization through the β-oxidation pathway. Interestingly, although the downregulation of ACSL4 was also able to inhibit the accumulation of lipid droplets, the reduction in the accumulation of lipid droplets did not affect the level of decidualization. This suggests that the accumulation of lipid droplets may be used for other physiological processes, such as storing energy for the embryo. Our study explored how ACSL4-mediated FA activation regulates endometrial decidualization through the β-oxidation pathway. This will provide interesting insights into the mechanism of lipid metabolism regulation during decidualization.

2. MATERIALS AND METHODS

2.1. Clinical samples

Human endometrial tissue samples (proliferative phase [n = 5], secretory phase [n = 9]) were obtained from the First Affiliated Hospital of Dalian Medical University after informed consent was obtained from patients in accordance with the guidelines of the Declaration of Helsinki. The characteristics of the participants are listed in Supplementary Table 1. Paraffin sections of endometrial tissue were identified by pathologists through hematoxylin-eosin staining. This project was approved by the Ethics Committee of the First Affiliated Hospital of Dalian Medical University (YJ-KY-FB-2021—13).

2.2. Mice experiments

Adult ICR mice (8—10 weeks old) were purchased from the Experimental Animal Center of Dalian Medical University. Mice were housed in a specific environment controlled by temperature and light (14 h of light/10 h of darkness) with free access to food and water. All animal experiments were reviewed and approved by the Animal Ethics Committee of Dalian Medical University (project approval no. AEE21086). For the pregnancy mouse model, mice were mated in cages the night before according to a 2:1 ratio for females: males. The females were examined the next morning for the formation of vaginal plugs. If a vaginal plug was present, it was defined as the first day (D1) of mating. Uterine tissue was collected during D2—D6 (peri-implantation). For a mouse intrauterine injection model, on D3, two small incisions were made in anesthetized mice at the muscular wall on either side of the dorsal midline (near the ovaries) to locate the

uterine—oviduct connecting region. Small interfering (siRNA) against *Acsl4* or a negative control (NC; scrambled siRNA) mixed with Lipofectamine 2000 (#11668019; Invitrogen, Carlsbad, CA, USA) and normal saline were injected into the lumen of each uterine horn. The mice were euthanized (sodium pentobarbital: 150 mg/kg intraperitoneal) on D7. Uteri were collected and embryos were observed for implantation. The interference sequences are shown in Supplementary Table 2. Artificially induced deciduoma models were performed according to a previous report [23].

2.3. Cell culture and treatments

Human ESCs were a gift from Prof. Wang Haibin of Xiamen University. Endometrial stromal cells were grown in DMEM/F12 medium containing 10% fetal bovine serum (FBS) and 1% penicillin and streptomycin, and cultured in an incubator at 37 °C with 5% CO_2. For the *in vitro* induced ESC decidualization model, ESCs were cultured in DMEM/F12 containing 2% FBS and treated with medroxyprogesterone acetate (MPA; 1 μM; #B1510; APExBIO Technology, Houston, TX, USA) and dibutyryl-cAMP (db-cAMP; 0.5 mM; #B9001, APExBIO) for 3, 5, and 7 days. The induction medium was changed every 2 days. Endometrial stromal cells induced to decidualization *in vitro* were treated with the carnitine palmitoyl transferase (CPT)1 inhibitor, etomoxir (25 μM, 50 μM; #HY-50202; MedChemExpress, Monmouth Junction, NJ, USA) for 24 h or 48 h; the diacylglycerol acyltransferase 2 (DGAT2) inhibitor, PF-06424439 (10 μM, 20 μM; #HY-108341A; MedChemExpress) for 24 h or 48 h; the DGAT1 inhibitor, PF-04620110 (5uM; #HY-13009; MedChemExpress) for 24 h; and CPT1 agonists, baicalin (25 μM, 50 μM; #HY-N0197; MedChemExpress), and C75 (1 μM, 4 μM; HY-12364, MedChemExpress) for 24 h, respectively. For siRNA experiments, 100 nM siRNA was transfected into cells using 5 μL Lipofectamine 2000 (#11668019, Invitrogen) and the cells were collected after 48 h. The interference sequences for targeted genes are shown in Supplementary Table 3.

2.4. Cell proliferation and migration assays

Cell proliferation/viability was detected using a Cell Counting Kit-8 (CCK-8; #K1018; APExBIO). Cells were inoculated into 96-well plates (5000 cells/well), 10 μL CCK-8 was added to each well, and cells were incubated for 2 h at 37 °C in an incubator. The absorbance was measured at 450 nm. For a migration assay, the induced decidualized cells were transfected with ACSL4 siRNA, and three straight lines were drawn with a 200 μL pipette tip. After incubation for 12 h, the wound gap was observed and photographed with a microscope (Nexcope, China).

2.5. Western blotting (WB) analysis

Total cellular proteins were extracted using lysis buffer (#KGB5303-100; KeyGEN BioTECH, Nanjing, China) which contains protease inhibitors, phosphatase inhibitors, and phenylmethyl-sulfonyl fluoride. Protein concentrations were measured by bicinchoninic acid assay kit (#P0011; Beyotime Biotechnology, Shanghai, China), followed by separation of protein samples by 10% or 12% SDS polyacrylamide gel electrophoresis. The proteins were then transferred to nitrocellulose membranes (#66485; Pall Corporation, Port Washington, NY, USA), which were then blocked with 5% skim milk powder. The membranes were incubated with antibodies overnight at 4 °C, which are ACSL4 (1:1000; #A20414; ABclonal, Wuhan, China), PRL (1:800; #A1618; Abclonal), IGFBP1 (1:1000; #A11109; Abclonal), FOXO1 (1:1000; #18592-1-AP; Proteintech, Wuhan, China), HOXA10 (1:1000; #26497-1-AP; Proteintech), CPT1A (1:1000; #A5307; Abclonal), CPT2 (1:1000; #A12426; Abclonal). The membranes were washed and then incubated with horseradish peroxidase-conjugated secondary antibodies (1:4000; #SA00001-1/2; Proteintech) for 1 h at room temperature. The visualization and analysis of bands were performed using chemiluminescent detection reagents (#180-5001; Tanon, Shanghai, China) and an image detection system (Tanon).

2.6. Quantitative polymerase chain reaction (qPCR) analysis

TRIzol reagent (#9109; Takara, Shiga, Japan) was used for the extraction of total cellular RNA. Copy DNA was synthesized using a Reverse Transcription Kit (#R223-01; Vazyme, Nanjing, China). A Real-Time PCR System (Thermo Fisher Scientific, Waltham, MA, USA) was used to analyze target genes using a Real-Time PCR Kit (#AQ131-04, Transgen, China) by quantitative polymerase chain reaction (qPCR). Differential changes were calculated by the $2^{-\Delta\Delta CT}$ method for raw data. Primer sequences are shown in Supplementary Table 4.

2.7. Immunohistochemistry (IHC) staining

Tissue paraffin sections were deparaffinized in gradient xylene. Endogenous peroxidase activity was quenched with 3% H_2O_2. Sections were blocked with 5% goat serum and incubated overnight at 4 °C with anti-ACSL4 antibody (1:200; #A2044; ABclonal), followed by a 2-h incubation at room temperature with biotinylated secondary antibody (#KIT-9720; MXB Biotechnologies, Fuzhou, China). Finally, diaminobenzidine was used for staining. Photographs were taken using a microscope (Nexcope, China), and images were analyzed by Image-Pro Plus software (Media Cybernetics, Rockville, MD, USA).

2.8. Phalloidin and BODIPY 493/503 staining

Cells were fixed with 4% paraformaldehyde, washed with phosphate buffered saline, and incubated with fluorescein isothiocyanate (FITC)-phalloidin (1:200; #RM02836; ABclonal) for 60 min, and then counterstained with DAPI (1:2000; C1002; Beyotime). Living cells were incubated with a BODIPY 493/503 staining kit (BODIPY493/503: Hoechst33342: assay Buffer = 1:1:1000, C2053S, Beyotime) for 15 min to visualize LDs. Then, the stained cells were photographed by a fluorescence microscope (Nexcope, Ningbo, China) and fluorescence intensity was analyzed using Image-Pro Plus software (Media Cybernetics).

2.9. ATP assays

Intracellular ATP levels were measured using an ATP assay kit (#BC0305; Solarbio, Beijing, China). The cells were collected in a centrifuge tube, the supernatant was discarded and an appropriate amount of extract buffer was added. The ATP level was measured in experiments performed according to the manufacturer's instructions.

2.10. Oxygen consumption rate (OCR) measurement

The OCR was assayed using an XFe24 extracellular flux analyzer (Seahorse Bioscience, Billerica, MA). According to previous reports [24—26], in brief, the treated cells were inoculated in XFe24 cell culture microtiter plates for 12 h before the experiment and then analyzed by OCR using the Cell Mito Stress Test Kit (103015-100, Seahorse Bioscience).

2.11. Statistical analysis

All data are expressed as mean ± standard deviation. A Student's *t*-test and one-way analysis of variance conducted by GraphPad Prism 8.0 (GraphPad Software, La Jolla, CA, USA) were used for differences analysis. $P < 0.05$ was considered statistically significant. Experiments were repeated three or more times.

3. RESULTS

3.1. The expression of ACSL4 increased during ESC decidualization

To determine the expression of ACSL4 in endometrial tissues, we used immunohistochemistry to detect the expression levels of ACSL4 protein in human endometrium during proliferative and secretory phases. We found that ACSL4 was highly expressed during the secretory phase (Figure 1A). Further, we investigated the expression level of ACSL4 during decidualization *in vitro*. Quantitative PCR results showed that mRNA levels of the decidualizing markers, insulin-like growth factor-binding protein 1 (IGFBP1), prolactin (PRL), forkhead box O1 (FOXO1), and homeobox A10 (HOXA10), gradually increased in human ESCs after MPA and db-cAMP treatments (Figure 1B). Similar results were also obtained in protein levels of decidualizing markers after MPA and db-cAMP treatments (Figure 1C). Immunofluorescence (IF) experiments with F-actin (FITC-phalloidin) showed that ESCs changed from a long shuttle shape to a large round shape (polygonal) after MPA and db-cAMP treatments (Figure 1D). The expression of ACSL4 was elevated during decidualization at both mRNA and protein levels (Figure 1B, C). Increased ACSL4 expression was also observed by IF (Figure 1E). Subsequently, we developed a pregnant mouse model and found that Acsl4 expression was the highest in the endometrium at D4 of gestation (Figure 1F). Taken together, these results suggest that ACSL4 is highly expressed during decidualization and may play an important role in this process.

3.2. Knockdown of ACSL4 impairs ESC decidualization

To determine whether ACSL4 affects the function of ESCs and participates in decidualization, we first knocked down the expression of ACSL4 in ESCs by small interfering (si)RNA (Figure 2A). We then measured cell viability by CCK-8 assay, we found that ESC proliferation was inhibited after the downregulation of ACSL4 (Figure 2B). To clarify the effect of ACSL4 on decidualization, we verified the decrease in ACSL4 mRNA and protein levels could be observed in decidual cells transfected with ACSL4 siRNA (Figure 2C, D). The inhibition of ACSL4 significantly reduced mRNA and protein levels of the decidualization markers, IGFBP1, PRL, FOXO1, and HOXA10 (Figure 2C, D). IF showed that the knockdown of ACSL4 eliminated the specialized phenotypic modification of ESCs during decidualization. The longitudinal orientation of F-actin filaments remained unaltered, and the transverse orientation became thinner and narrower (Figure 2E). Interestingly, scratch experiments found that induced decidualization inhibited ESC migration, while downregulation of ACSL4 reversed this phenomenon (Figure 2F). To validate the migration results, we examined the protein expression of the epithelial cell marker E-cadherin and mesenchymal cell marker N-cadherin and found that knockdown of ACSL4 inhibited mesenchymal to epithelial transition induced by MPA and db-cAMP in ESCs (Figure 2G). This also verified the effect of the downregulation of ACSL4 on ESC morphology (Figure 2E). To further validate the effect of Acsl4 deletion on embryo implantation, we injected an NC (scrambled siRNA) and Acsl4 siRNA into the uterine horns and assessed the efficiency of embryo implantation. The result showed that the downregulation of Acsl4 was found to inhibit embryo implantation (Figure 2H). Subsequently, we also verified the downregulation efficiency in the endometrium that had been injected with Acsl4 siRNA (Figure 2I), and the implantation efficiency of the siAcsl4 group was significantly lower than that of the control group (Figure 2J). These findings suggest that the knockdown of ACSL4 inhibits the decidual process of ESCs and that ACSL4 plays an indispensable role in ESC decidualization.

3.3. Knockdown of ACSL4 inhibits lipid droplet accumulation and FA β-oxidation during ESC decidualization

Considering that intracellular FA activation may enter catabolism and/or anabolism, in order to determine the potential mechanisms of ACSL4 in regulating decidualization, we examined lipid droplet synthesis and FA β-oxidation during the decidual process, respectively (Figure 3A). First, through BIODIPY 493/503 staining (strong fluorescence in lipid-rich environments), we found a gradual accumulation of lipid droplets during decidualization (Figure 3B), which is consistent with the findings of Tamura et al. [11]. Moreover, glycerol-sn-3-phosphate acyltransferase 4 (GPAT4, which is widely expressed in various human tissues [27], and is the first step in the synthesis of TAG, catalyzes glycerol-3-phosphate acylated to form 1-acyl-G3P) and DGAT2 (which catalyzes the esterification of diacylglycerol to form TAG) are two key enzymes for TAG synthesis (Figure 3A), and their mRNA expressions were increased (Figure 3C). Further, knockdown of ACSL4 inhibited the accumulation of lipid droplets, and the expression of GPAT4 and DGAT2 during the decidual process (Figure 3D, E). In addition, the detection of CPT1A (located in the outer membrane of the mitochondria, catalyzes the reversible binding of fatty acyl-CoA [12 to 18 carbon chain lengths] to L-carnitine), and CPT2 (located in the inner mitochondrial membrane, releases fatty acyl-CoA into the mitochondrial matrix), the key enzymes of β-oxidation (Figure 3A), showed that levels of CPT1A and CPT2 proteins increased after MPA and db-cAMP induced ESCs (Figure 3F). Similar results were also obtained at the levels of CPT1A and CPT2 mRNA (Figure 3G). The ATP levels increased during the decidualization of ESCs (Figure 3H). To further clarify the level of FA β-oxidation during decidualization, we analyzed the mitochondrial OCR with the Seahorse Extracellular Flux Analyzer (Figure 3I). The results showed that the basal respiration (Figure 3J) and ATP production (Figure 3K) of decidual cells were higher. Furthermore, the downregulation of ACSL4 inhibited the protein and mRNA expression of CPT1A and CPT2 during the decidual process (Figure 3L, M), and also inhibited ATP production of decidual cells by observing the OCR (Figure 3K). These results suggest that lipid droplet accumulation and β-oxidation are enhanced in decidual cells, while the downregulation of ACSL4 may inhibit lipid droplet accumulation and FA β-oxidation levels during the decidual process.

3.4. Inhibition of FA β-oxidation decreased ESC decidualization levels

To elucidate whether ACSL4-activated fatty acyl-CoA affects the decidual process through anabolism or catabolism, we observed ESC decidualization after the inhibition of β-oxidation and TAG synthesis, respectively. First, we treated ESCs with etomoxir (pharmacological inhibition of FA β-oxidation by inhibiting the entry of long-chain FAs into mitochondria via blocking CPT1 activity [28]). We found that 25 μM and 50 μM of etomoxir for 24 h or 48 h were able to reduce ATP production (Figure 4A). Further, we found that etomoxir was able to inhibit MPA and db-cAMP-induced elevated expressions of IGFBP1, PRL, FOXO1, and HOXA10 mRNA (Figure 4B). Similar results were observed at the protein level (Figure 4C). In addition, IF also showed that etomoxir inhibited morphological changes in decidual cells (Figure 4D). To further demonstrate the effect of inhibition of β-oxidation on decidualization, we also used the siRNA of CTP1A as reported previously [29] and verified its interference efficiency (Figure 4E). We found that the downregulation of CPT1A reduced MPA and db-cAMP-induced elevated expressions of IGFBP1, PRL, FOXO1, and HOXA10 at both mRNA and protein levels (Figure 4F, G). The observation of cell morphology by F-actin staining also showed that

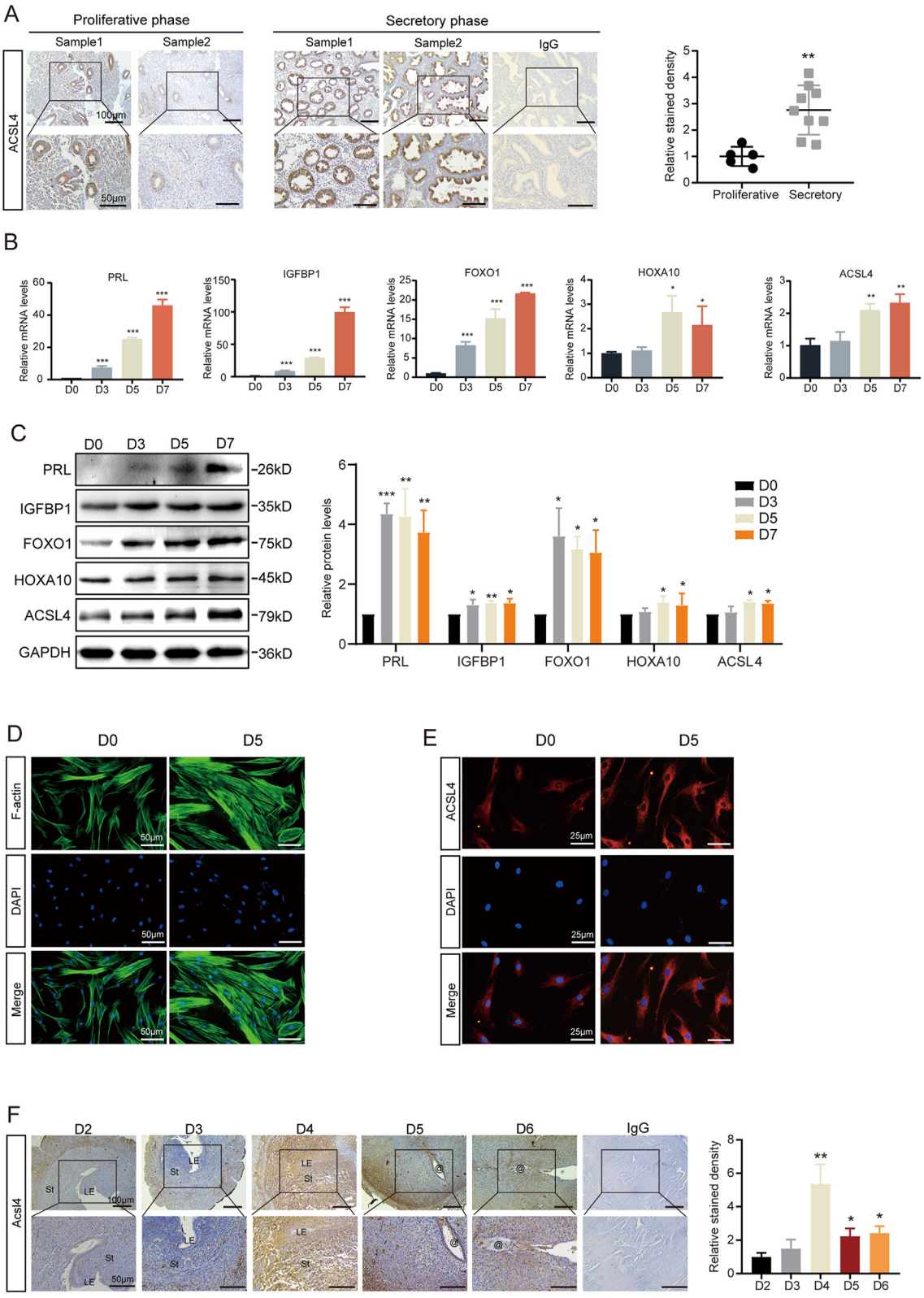

Figure 1: The expression of ACSL4 during the ESC decidualization. A. IHC detected the expression of ACSL4 in human endometrial tissues during the proliferative phase (n = 5) and secretory phase (n = 9), scale bar = 100 μm/50 μm, *vs. proliferative phase. The ESCs were treated with 1 μM MPA and 0.5 mM db-cAMP for 3, 5, and 7 days, and then qPCR (B, normalized by GAPDH) or WB (C) was performed to detect the expressions of PRL, IGFBP1, HOXA10, FOXO1 and ACSL4, *vs. D0. The ESCs were treated with 1 μM MPA and 0.5 mM db-cAMP for 3, 5, and 7 days, and FITC-phalloidin staining (D, scale bar = 50 μm) was performed to detect the F-actin and IF (E, scale bar = 25 μm) was performed to detect ACSL4 expression. F. IHC detected the expression of Acsl4 on D2-D6 uterine tissues of the pregnant mouse model, LE: luminal epithelium; St: stroma; @: embryo; scale bar = 100 μm/50 μm, *vs. D2. $*p < 0.05$, $**p < 0.01$, $***p < 0.001$.

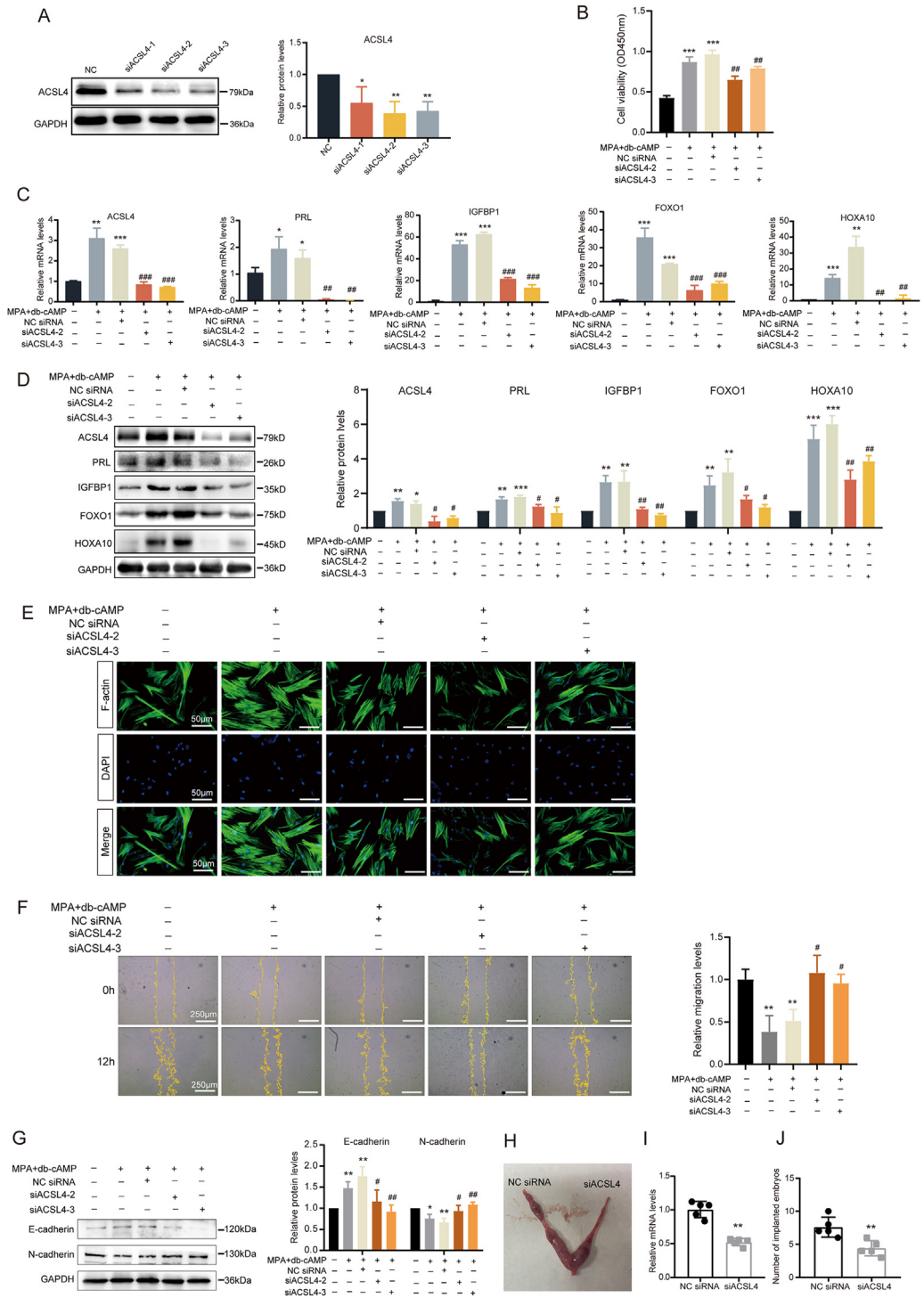

Figure 2: Downregulation of ACSL4 inhibits the ESC decidualization. A. WB was used to detect the knockdown effect of three interference sequences on ACSL4, *vs. NC. B. CCK-8 was used to detect cell proliferation after transfection with ACSL4 siRNA, *vs. NC, #vs. MPA + db-cAMP + NC siRNA. qPCR (C, normalized by GAPDH) and WB (D) were used to detect the expression levels of PRL, IGFBP1, HOXA10, FOXO1 and ACSL4 in MPA and db-cAMP-induced ESCs which were transfected with ACSL4 siRNA, *vs. NC, #vs. MPA + db-cAMP + NC siRNA. E. FITC-phalloidin staining was performed to detect the F-actin expression in MPA and db-cAMP-induced ESCs which were transfected with ACSL4 siRNA, scale bar = 50 μm. F. Scratch experiments were performed to detect the migration of induced ESCs which were transfected with ACSL4 siRNA, scale bar = 250 μm, *vs. NC, #vs. MPA + db-cAMP + NC siRNA. G. WB was used to detect the expression levels of E-cadherin and N-cadherin of induced ESCs which were transfected with ACSL4 siRNA, *vs. NC, #vs. MPA + db-cAMP + NC siRNA. H. Representative photograph of the mouse uterus after injection of Acsl4 siRNA. I. The qPCR was used to detect the expression of Acsl4 in the endometrium of mice (NC siRNA as control) after injecting Acsl4 siRNA into the uterine horn, normalized by GAPDH, *vs. NC. J. Implantation efficiency of the embryo after the injection of Acsl4 siRNA into the uterine horn, n = 5, *vs. NC. $*p < 0.05$, $**p < 0.01$, $***p < 0.001$. $\#p < 0.05$, $\#\#p < 0.01$, $\#\#\#p < 0.001$.

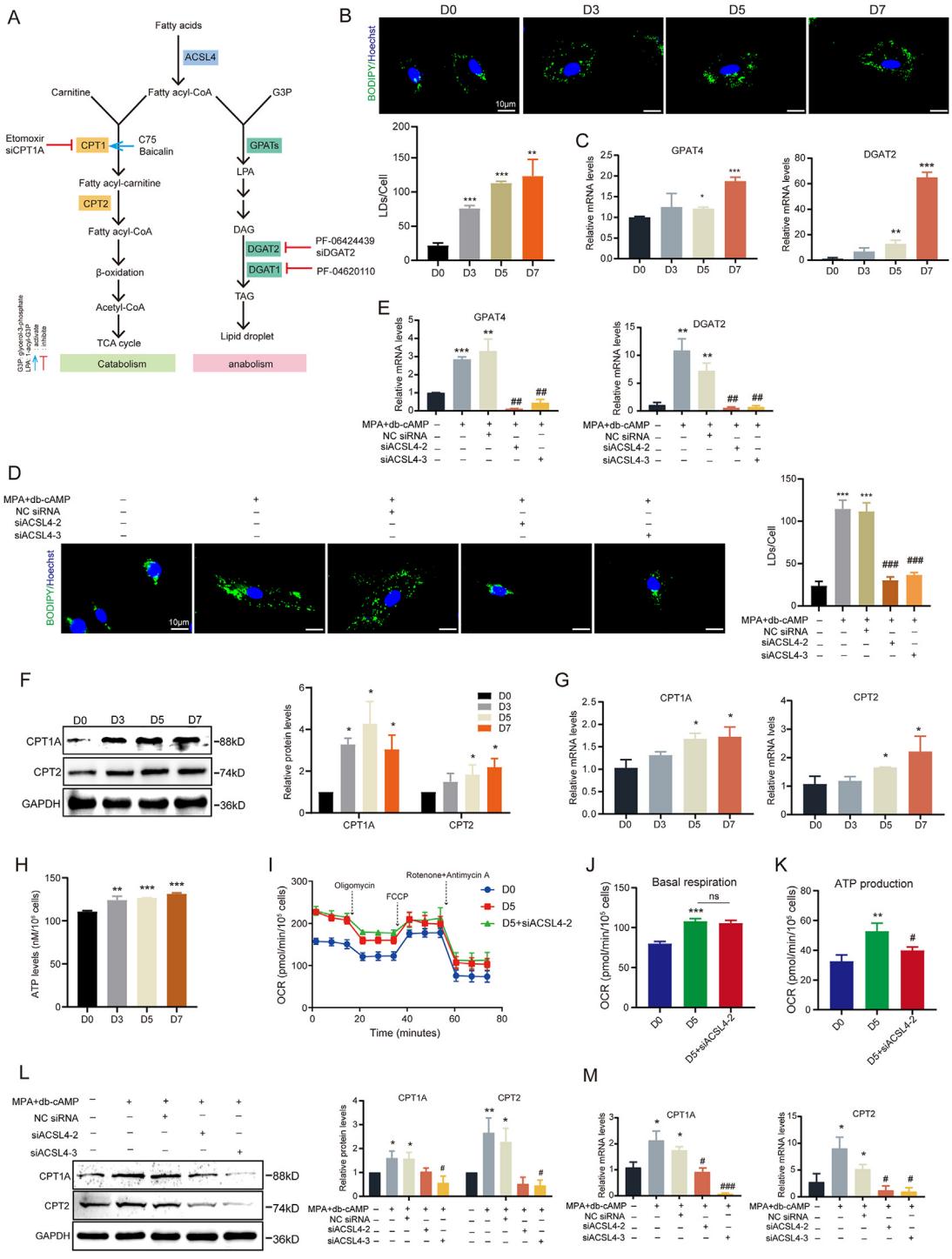

Figure 3: Downregulation of ACSL4 inhibits FA β-oxidation and lipid droplet synthesis. A. Pattern diagram of fatty acid activation through ACSL4 into anabolism and catabolism. The ESCs were treated with 1 μM MPA and 0.5 mM db-cAMP for 3, 5, and 7 days, and intracellular lipid droplet levels were detected by BIODIPY 493/503 staining (B, scale bar = 10 μm), and the mRNA expression of GDAT2 and GPAT4 was detected by qPCR (C, normalized by GAPDH), *vs. D0. After MPA and db-cAMP-induced ESCs were transfected with ACSL4 siRNA, BIODIPY 493/503 staining (D, scale bar = 10 μm) was used to detect lipid droplet levels, qPCR (E, normalized by GAPDH) was used to detect the CPT1A, CPT2 mRNA expression, *vs. NC, #vs. MPA + db-cAMP + NC siRNA. The ESCs were treated with 1 μM MPA and 0.5 mM db-cAMP for 3, 5, and 7 days, and then WB (F) or qPCR (G, normalized by GAPDH) was performed to detect the expression of CPT1A, CPT2, *vs. D0. H. The ESCs were treated with 1 μM MPA and 0.5 mM db-cAMP for 3, 5, and 7 days, and ATP levels were detected by ATP assay kit, *vs. D0. I. The OCR was detected after MPA and db-cAMP-induced ESCs which were transfected with or without ACSL4 siRNA. J. Basal respiration, Basal respiration was calculated as the three OCR measurements before the addition of oligomycin minus the three OCR measurements after the addition of rotenone and antimycin A, *vs. D0. K. ATP production, ATP production was calculated as the three OCR measurements before oligomycin injection minus the three OCR measurements after oligomycin injection, *vs. D0, #vs. D5. After MPA and db-cAMP-induced ESCs were transfected with ACSL4 siRNA, WB (L) or qPCR (M, normalized by GAPDH) was performed to detect the expression of CPT1A, CPT2, *vs. NC, #vs. MPA + db-cAMP + NC siRNA. $^{*}p < 0.05$, $^{**}p < 0.01$, $^{***}p < 0.001$, $\#p < 0.05$, $\#\#p < 0.01$, $\#\#\#p < 0.001$.

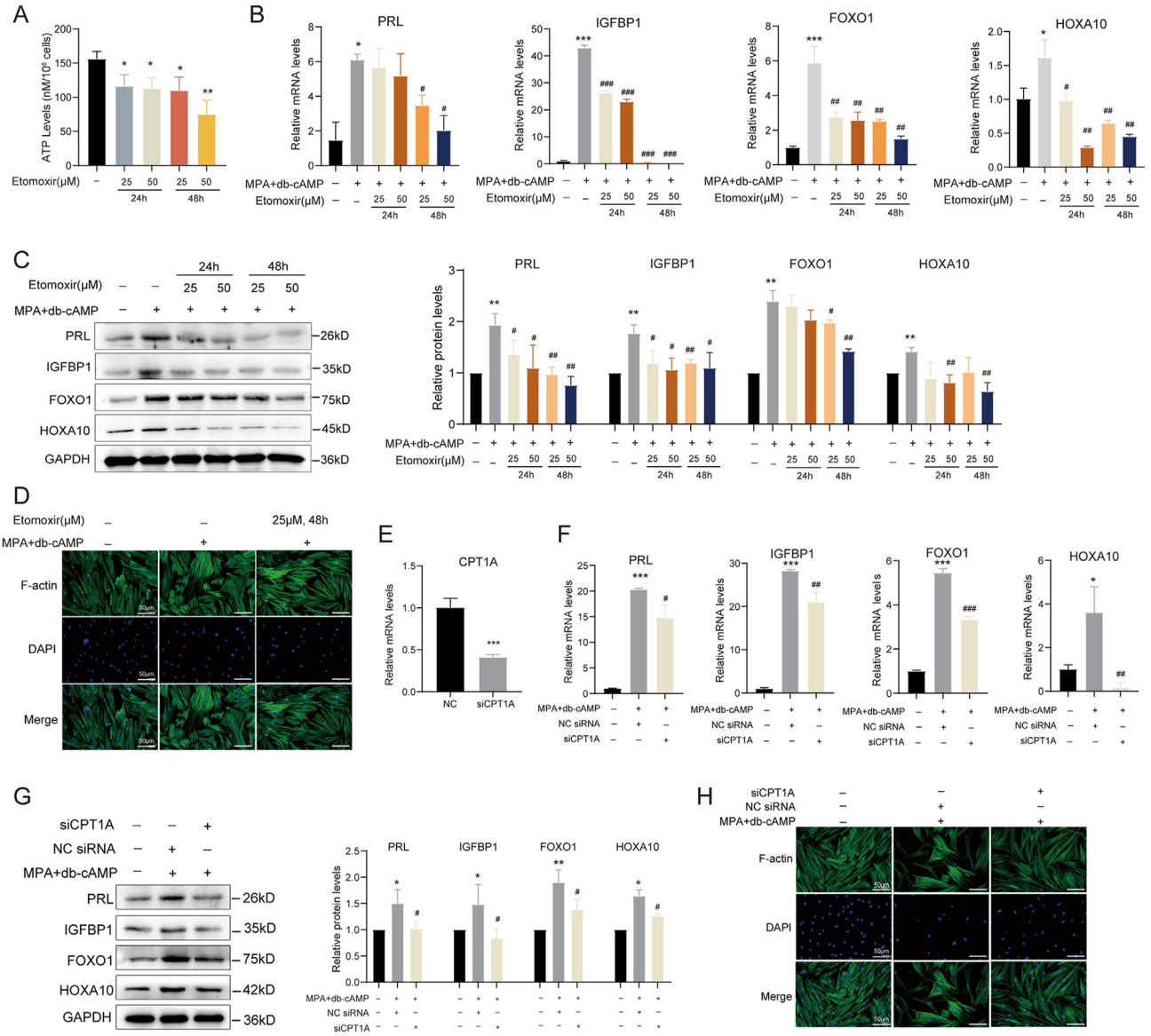

Figure 4: Inhibition of FA β-oxidation impairs decidualization. A. The ESCs were treated with 25 μM and 50 μM etomoxir for 24 or 48 h, and then the ATP level was detected by ATP assay kit, *vs. NC. After MPA and db-cAMP-induced ESCs were treated with 25 μM, 50 μM etomoxir for 24 or 48 h, qPCR (B, normalized by GAPDH) or WB (C) were performed to detect the expression of PRL, IGFBP1, HOXA10, FOXO1, *vs. NC, #vs. MPA + db-cAMP. D. After MPA and db-cAMP-induced ESCs were treated with 25 μM etomoxir for 48 h, FITC-phalloidin staining was performed to detect the F-actin expression, scale bar = 50 μm. E. The interference efficiency of the ESCs which were transfected with CPT1A siRNA was verified by qPCR, normalized by GAPDH, *vs. NC. After MPA and db-cAMP-induced ESCs were transfected with CPT1A siRNA, qPCR (F, normalized by GAPDH) or WB (G) was performed to detect the expression of PRL, IGFBP1, HOXA10, FOXO1, and FITC-phalloidin staining (H, scale bar = 50 μm) was performed to detect the F-actin expression, *vs. NC, #vs. MPA + db-cAMP. *$p < 0.05$, **$p < 0.01$, ***$p < 0.001$, #$p < 0.05$, ##$p < 0.01$, ###$p < 0.001$.

siCPT1A eliminated the specialized phenotypic modification of decidual cells (Figure 4H). These results demonstrate the importance of FA β-oxidation to decidualization and also suggest that it may affect the decidual process by ACSL4-mediated catabolism.

3.5. Inhibition of lipid droplet accumulation does not affect ESC decidualization

To determine the effect of lipid droplet accumulation on decidualization, we performed BIODIPY 493/503 staining of ESCs after treatment with PF-06424439, a selective inhibitor of DGAT2 [30], for 24 h or 48 h. Since DGAT2 plays a role in esterifying both endogenous and exogenous FAs, whereas DGAT1 preferentially acylates exogenous FAs and has the additional important role of re-esterifying DAGs and monoacylglycerols from the hydrolysis of existing lipid droplets [31,32], we gave priority to inhibiting lipid drop synthesis by inhibiting DGAT2. We found that 10 μM or 20 μM PF-06424439 inhibited the accumulation of lipid droplets during an induced ESC decidual process (Figure 5A). Interestingly, PF-06424439 did not reduce the protein expression of IGFBP1, PRL, FOXO1, and HOXA10 (Figure 5B). F-actin fluorescence also showed that the inhibition of lipid droplet accumulation by PF-06424439 did not affect the morphology of decidual cells (Figure 5C). Subsequently, we verified these results by genetically downregulating DGAT2. The downregulation efficiency of DGAT2 siRNA showed that the two sequences designed by us were effective in decreasing DGAT2 mRNA

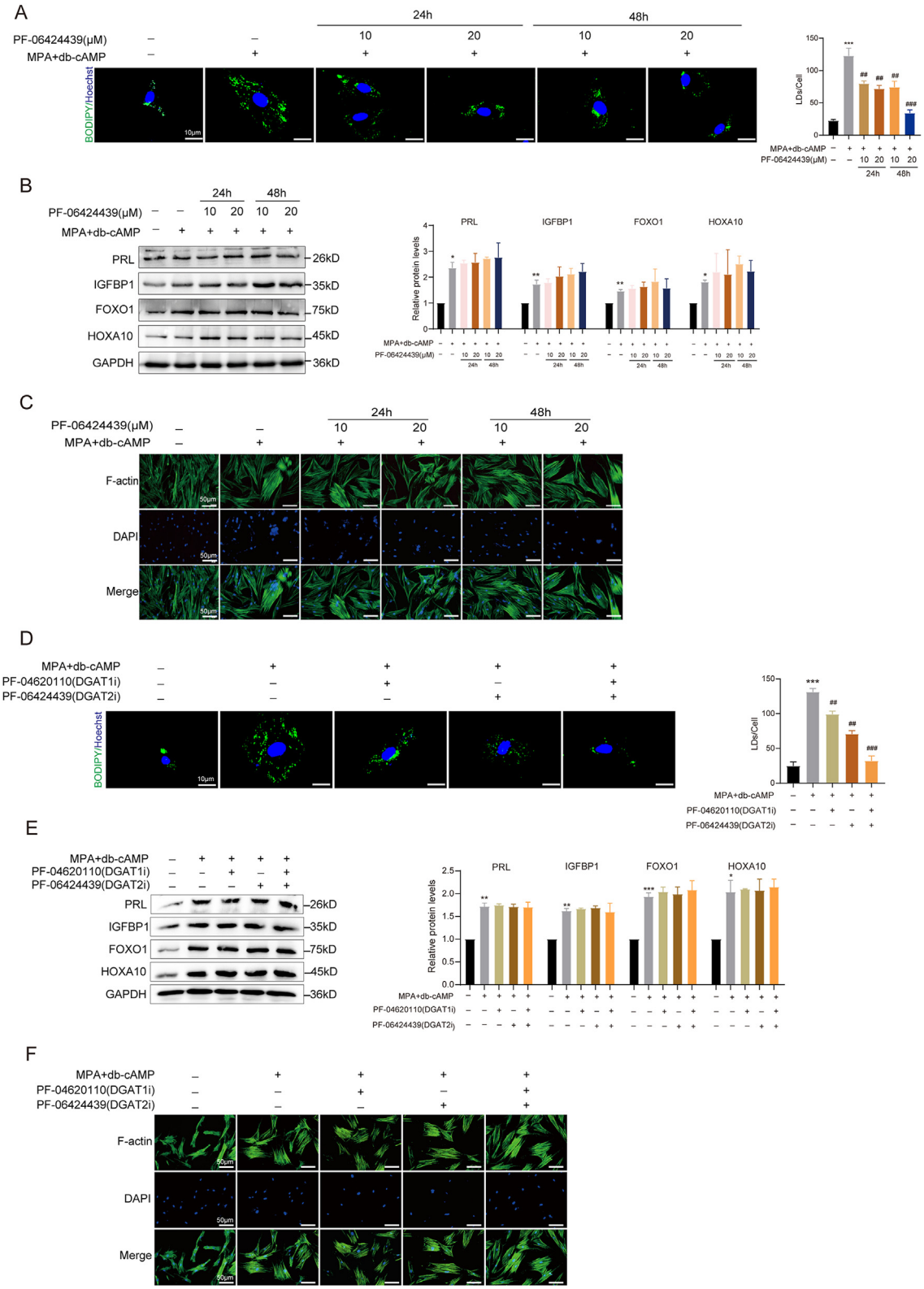

Figure 5: Inhibition of lipid droplet accumulation did not affect decidualization. After MPA and db-cAMP-induced ESCs were treated with 10 μM, 20 μM FP-06424439 for 24 or 48 h, the BIODIPY 493/503 staining (A, scale bar = 10 μm) was used to detect lipid droplet levels, WB (B) was performed to detect the expression of PRL, IGFBP1, HOXA10, FOXO1, and FITC-phalloidin staining (C, scale bar = 50 μm) was performed to detect the F-actin expression, *vs. NC, #vs. MPA + db-cAMP. After MPA and db-cAMP-induced ESCs were treated with FP-06424439 (10 μM) or/and PF-04620110 (5 μM) for 48 h, the BIODIPY 493/503 staining (D, scale bar = 10 μm) was used to detect lipid droplet levels, WB (E) was performed to detect the expression of PRL, IGFBP1, HOXA10, FOXO1, and FITC-phalloidin staining (F, scale bar = 50 μm) was performed to detect the F-actin expression, *vs. NC, #vs. MPA + db-cAMP. *$p < 0.05$, **$p < 0.01$, ***$p < 0.001$, #$p < 0.05$, ##$p < 0.01$, ###$p < 0.001$.

expression (Supplementary Figure 1A). The downregulation of DGAT2 inhibited the accumulation of lipid droplets during the ESC decidual process (Supplementary Figure 1B). Similar to findings in a pharmacological inhibitor, the knockdown of DGAT2 did not affect the expression of IGFBP1, PRL, FOXO1, and HOXA10 (Supplementary Figure 1C), as well as cellular morphological changes (Supplementary Figure 1D). Considering the possible role of DGAT1 and the influence of inhibiting lipid droplet synthesis on decidualization, we inhibited DGAT1 [33] while inhibiting DGAT2. The results showed that inhibition of DGAT2 and DGAT1 sufficiently suppressed lipid droplet synthesis (Figure 5D), but did not affect the expression of decidual marker molecules (Figure 5E) and cell morphology (Figure 5F). This indicates that although lipid droplet accumulation is increased during the decidual process, it is not associated with ACSL4-mediated decidualization and does not affect decidualization, suggesting that lipid droplet accumulation may be involved in other processes of embryo implantation (for example, maybe storing energy for the embryo).

3.6. ACSL4 regulates decidualization through FA β-oxidation pathway

Since simultaneously enhanced lipid droplet accumulation and β-oxidation suggested possible crosstalk in the intense lipid metabolism during the decidual process, we sought to elucidate the association between β-oxidation and lipid droplet accumulation. Interestingly, we found that the inhibition of lipid droplet synthesis by the inhibition of DGAT2, either pharmacologically or genetically, did not affect the protein expression levels of CPT1A and CPT2, as well as the ATP level during the induced ESC decidual process (Figure 6A—D). Furthermore, through the detection of mitochondrial OCR (Figure 6E), it was found that neither inhibition of DGAT2 (DGAT2 i) nor inhibition of both DGAT2 and DGAT1 (DGAT1 i) affected basal respiration and ATP production of decidual cells (Figure 6F, G). This suggests that inhibition of lipid droplet synthesis may not affect FA β-oxidation. Also, this would appear to explain why the inhibition of lipid droplet synthesis did not affect decidualization since we did not observe an elevation of FA β-oxidation. However, we found that inhibition of FA β-oxidation increased lipid droplet accumulation during the decidual process, as well as the mRNA expression level of DGAT2, through the pharmacological and genetic inhibition of CPT1A (Figure 6H—K). This partially explains why the increase in lipid droplet accumulation did not affect decidualization. To clarify whether ACSL4 affects ESC decidualization by activating FA β-oxidation, we pharmacologically or genetically inhibited CPT1A after the overexpression of ACSL4 in MPA- and db-cAMP-induced ESCs. We found that although ACSL4 was able to increase the expression of IGFBP1, PRL, FOXO1, and HOXA10, as well as to promote the transformation of cells to round, enlarged cells, the inhibition of CPT1A was able to eliminate these effects (Figure 6L—N). Studies have shown that C75 can pharmacologically activate CPT1 activity and enhance FA β-oxidation [34—36]. Therefore, we used C75 to treat ESCs. We found that the decreased expression of IGFBP1, PRL, FOXO1, HOXA10 proteins, and cell morphological changes induced by ACSL4 knockdown, could be partially reversed by C75 (1 μM, 4 μM; Figure 7A—C). However, because of the controversial activation mechanism of C75, which is also capable of acting as an inhibitor of fatty acid synthase [37—39], we repeated the relevant experiments using a newly discovered natural allosteric activator of CPT1A, baicalin (activating CPT1A activity accelerates the entry of long-chain fatty acyl-CoA into mitochondria for β-oxidation [40]) and obtained results consistent with those of C75. Baicalin rescued the expression decrease of IGFBP1, PRL, FOXO1, HOXA10, and cell morphological changes caused by downregulated ACSL4 (Figure 7D—F). For *in vivo* evidence, we established artificially induced deciduoma in ovariectomized female mice according to the previously reported protocol (Figure 7G). ACSL4 siRNA and baicalin were also injected into the uterine horn of mice while sesame oil induced decidualization. As shown in Figure 7H, the sesame oil-induced deciduoma was greater than that of the non-induced group, the deciduoma of the ACSL4 siRNA and the baicalin-injected group was greater than that of the ACSL4 siRNA group, and uterine horn weight measurements confirmed the positive effect of baicalin on deciduoma (Figure 7I). Further, the detection of IGFBP1, PRL, FOXO1, and HOXA10 in deciduoma tissue showed that baicalin could promote the expression of decidualization marker molecules after the downregulation of ACSL4 (Figure 7J), which further proved that baicalin promoted decidualization. Taken together, these results suggest that ACSL4-mediated FA activation promotes ESC decidualization through a β-oxidation pathway.

4. DISCUSSION

Long-chain FAs, which are abundant in mammals, are important nutrients involved in cell membrane structure, signal transduction pathways, energy metabolism, and other physiological functions. Long-chain FAs are converted by ACSLs to their respective acyl-CoA forms and thus enter anabolism and/or catabolism. Abnormal anabolism and catabolism caused by the dysregulation of FA metabolism may lead to various pathological processes [41,42]. Compared with the other four subtypes, ACSL4 is found in the adrenal gland, epididymis, seminal vesicle, ovary, liver, and many other tissues [17,42]. Subcellular localization revealed that ACSL4 was able to localize in mitochondria and the endoplasmic reticulum, which may be responsible for TAG synthesis and β-oxidation [43,44]. Recent studies have shown that the activation of long-chain FAs by ACSL4 can initiate many intracellular lipid metabolism pathways [22,45] and that the abnormal expression of ACSL4 is closely related to a variety of biological processes. ACSL4 is involved in the release of AA into the mitochondrial lumen to regulate steroid production [22,46]. ACSL4 activates PUFAs so that cancer cells become sensitive to ferroptosis [47,48]. In hepatocellular carcinoma, ACSL4 regulates de novo lipogenesis by accumulating TAG, cholesterols, and lipid droplets [21]. In addition, the study by Cho et al. showed that significant morphological changes were found in the uterine tissues of ACSL4-deficient female heterozygous mice, they became pregnant less often and had a reduced litter size [49]. This suggests that ACSL4 may regulate female fertility but the role of ACSL4 in the endometrium remains largely unknown.

In this study, using IHC staining of human and mouse endometrial tissues, we found that ACSL4 expression was elevated during the secretory and implantation phases. It is noteworthy that ACSL4 expression was higher in human endometrial epithelial cells, which was consistent with the results of Hu et al. [50]. ACSL4 was highly expressed in both epithelial and stromal cells in mouse endometrial tissues. This difference in subcellular localization between species is interesting, suggesting that ACSL4 may be important in human endometrial glands that secrete lipid droplets into the uterine lumen through the glandular epithelium. In addition, by iTRAQ proteomic analysis of endometrial tissues, Hu et al. found that ACSL4 acted as a potential regulator of endometrial receptivity [50]. The downregulation of ACSL4 led to decreased expression of endometrial receptivity markers (HOXA10, cyclooxygenase 2, leukemia inhibitory factor). Although both studies have shown that the knockdown of ACSL4 reduces implantation efficiency, in contrast to Hu et al., we believe that ACSL4 also plays a key role in the decidual process. This is because the expression of ACSL4 increases during the induction of ESC

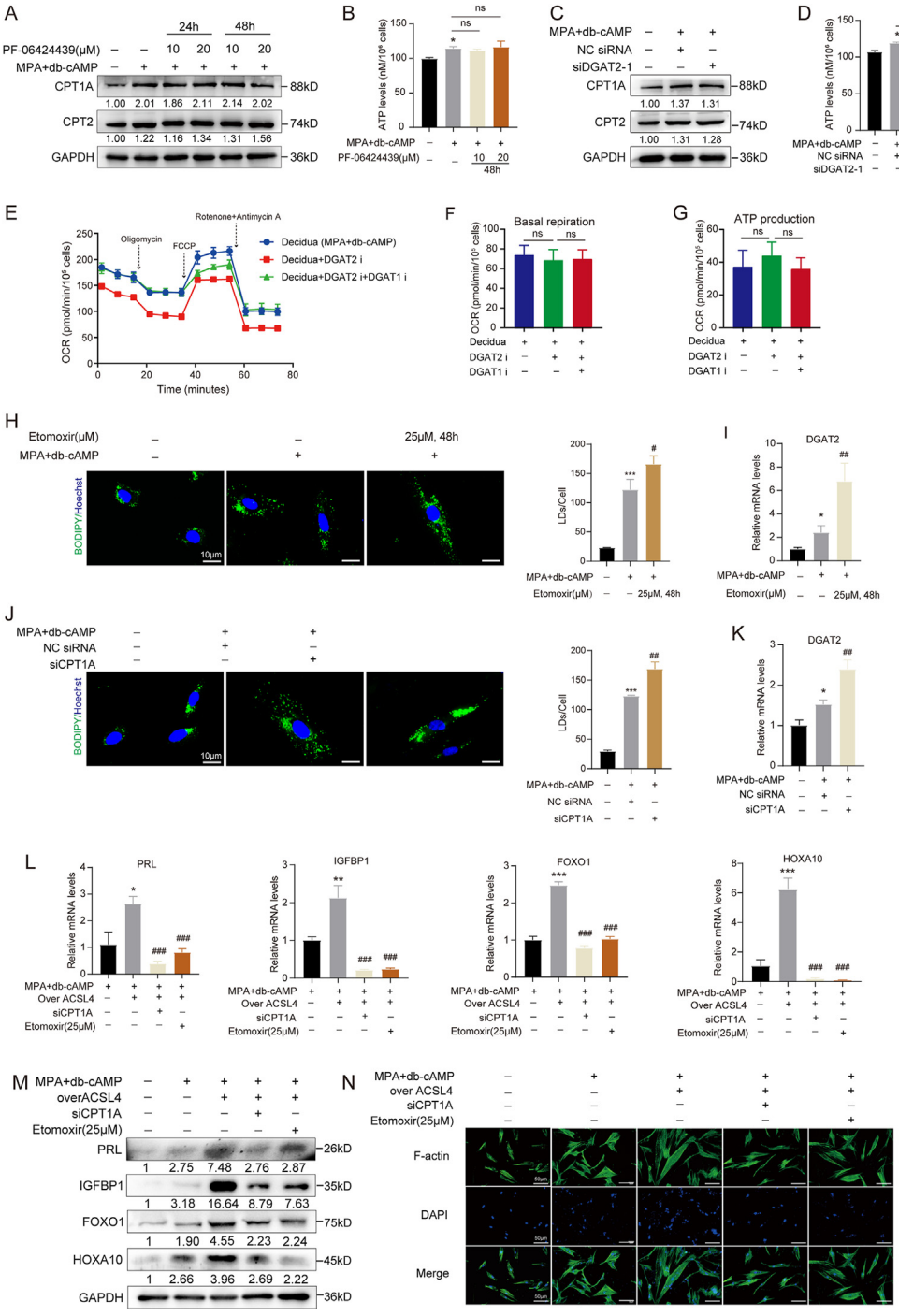

Figure 6: Inhibition of FA β-oxidation promotes lipid droplet accumulation. After MPA and db-cAMP-induced ESCs were treated with 10 μM, 20 μM FP-06424439 for 24 or 48 h, WB (A) was performed to detect the expression of CPT1A, CPT2, and ATP assay kit (B) was used to detect ATP level, *vs. NC. After MPA and db-cAMP-induced ESCs were transfected with DGAT2 siRNA, and WB (C) was performed to detect the expression of CPT1A, CPT2, and ATP assay kit (D) was used to detect ATP level, *vs. NC. E. The OCR was detected after MPA and db-cAMP-induced ESCs were treated with DGAT2 inhibitor PF-06424439 (20 μM) or/and DGAT1 inhibitor PF-04620110 (5 μM). F. Basal respiration, Basal respiration was calculated as the three OCR measurements before the addition of oligomycin minus the three OCR measurements after the addition of rotenone and antimycin A. G. ATP production, ATP production was calculated as the three OCR measurements before oligomycin injection minus the three OCR measurements after oligomycin injection. After MPA and db-cAMP-induced ESCs were treated with 25 μM etomoxir for 48 h, BIODIPY 493/503 staining (H, scale bar = 10 μm) was used to detect lipid droplet levels, and qPCR (I, normalized by GAPDH) was performed to detect the DGAT2 expression, *vs. NC, #vs. MPA + db-cAMP. After MPA and db-cAMP-induced ESCs were transfected with CPT1A siRNA, BIODIPY 493/503 staining (J, scale bar = 10 μm) was used to detect lipid droplet levels, and qPCR (K, normalized by GAPDH) was performed to detect the DGAT2 expression, *vs. NC, #vs. MPA + db-cAMP + NC siRNA. After MPA and db-cAMP-induced ESCs were transfected with OverACSL4 plasmid and treated with CPT1A siRNA or 25 μM etomoxir for 48 h, qPCR (L, normalized by GAPDH) or WB (M) was performed to detect the expression of PRL, IGFBP1, HOXA10, FOXO1, and FITC-phalloidin staining (N, scale bar = 50 μm) was performed to detect the F-actin expression, *vs. MPA + db-cAMP, #vs. MPA + db-cAMP + OverACSL4. *$p < 0.05$, **$p < 0.01$, **$p < 0.001$, #$p < 0.05$, ##$p < 0.01$, ###$p < 0.001$.

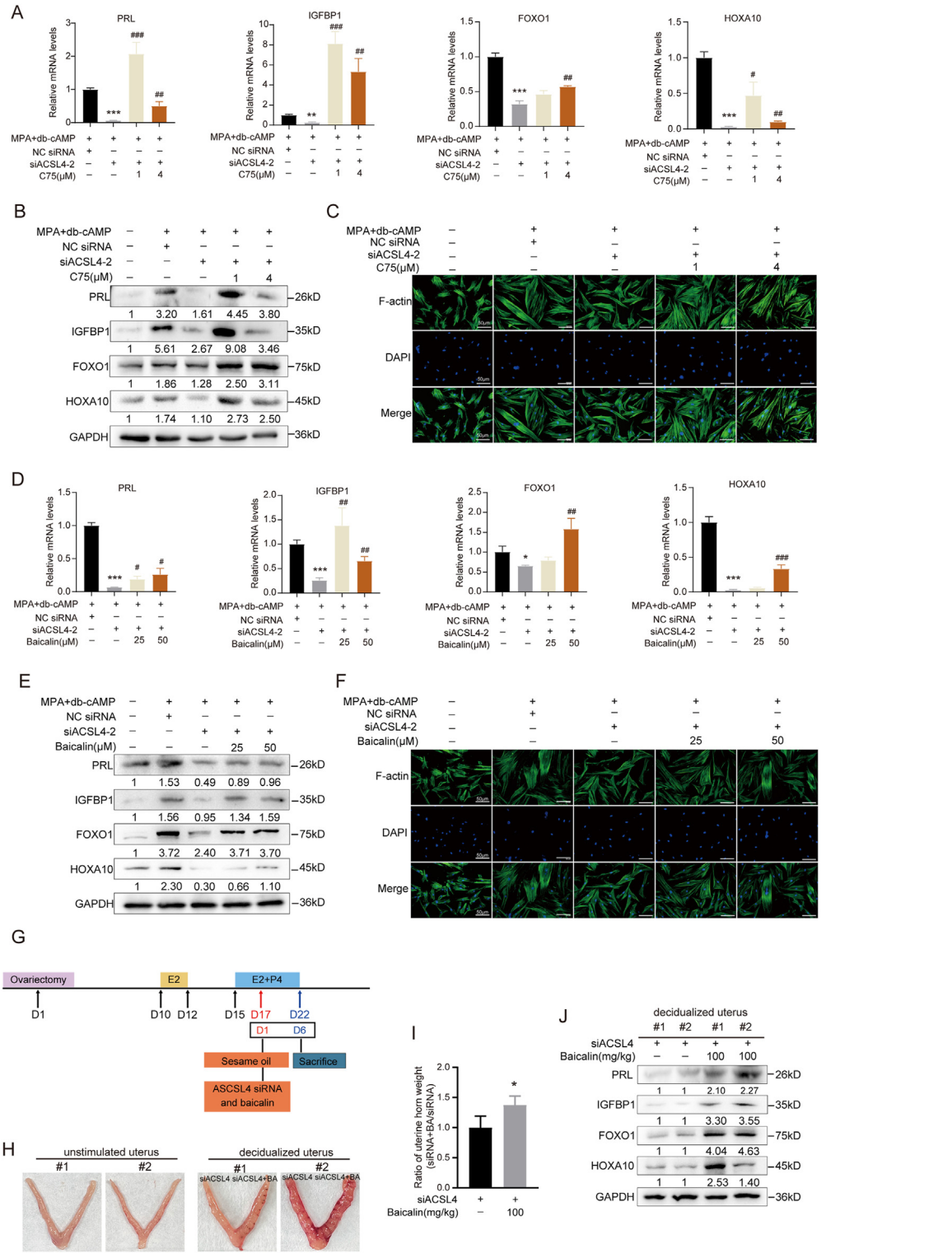

Figure 7: ACSL4 activates FA β-oxidation to promote decidualization. After MPA and db-cAMP-induced ESCs were transfected with ACSL4 siRNA and treated with 1 μM or 4 μM C75 for 24 h, qPCR (A, normalized by GAPDH) or WB (B) was performed to detect the expression of PRL, IGFBP1, HOXA10, FOXO1, and FITC-phalloidin staining (C, scale bar = 50 μm) was performed to detect the F-actin expression, *vs. MPA + db-cAMP + NC siRNA, #vs. MPA + db-cAMP + siACSL4-2. After MPA and db-cAMP-induced ESCs were transfected with ACSL4 siRNA and treated with 25 μM or 50 μM baicalin for 24 h, qPCR (D, normalized by GAPDH) or WB (E) was performed to detect the expression of PRL, IGFBP1, HOXA10, FOXO1, and FITC-phalloidin staining (F, scale bar = 50 μm) was performed to detect the F-actin expression, *vs. MPA + db-cAMP + NC siRNA, #vs. MPA + db-cAMP + siACSL4-2. G. Pattern diagram of artificially induced deciduoma which was treated with ACSL4 siRNA and baicalin (100 mg/kg). H. Representative picture of mouse deciduoma, BA: baicalin. I. Mouse uterine horns were weighed and normalized to the ACSL4 siRNA-injected group, n = 4, *vs. ACSL4 siRNA. J. WB was performed to detect the expression of PRL, IGFBP1, HOXA10, FOXO1 in deciduoma tissue, n = 4. *$p < 0.05$, **$p < 0.01$, ***$p < 0.001$, #$p < 0.05$, ##$p < 0.01$, ###$p < 0.001$.

decidua. Further, the knockdown of ACSL4 inhibits the expression of the decidualization markers, IGFBP1, PRL, FOXO1 and HOXA10, and changes cytoskeletal morphology. These findings suggest that ACSL4 is involved in the regulation of decidualization and is crucial for its occurrence. In terms of mechanism, we speculate that this may be caused by anabolism and/or catabolism mediated by the activation of FAs in which ACSL4 is involved.

Evidence in the last 20 years has revealed the important role of lipid metabolism in embryo implantation and endometrial receptivity [8]. For example, some FAs may induce endometrial inflammatory responses by mediating prostaglandin production and thus promote pregnancy [51]. Phospholipid-derived mediators, such as endocannabinoids, are associated with endometrial receptivity and decidualization [52]. Steroid hormones regulate uterine structure and function [53]. Given the importance of lipid metabolism for embryo implantation, a better understanding of lipid metabolism may have important clinical implications for the diagnosis and protection of female reproduction. Activated FAs are either broken down into acetyl-CoA by catabolism and then enter the tricarboxylic acid (TCA) cycle to help ATP production, or are converted into TAG, phospholipids, cholesterol lipids, and other metabolites by anabolism and stored in lipid droplets. Previous studies have reported that lipid droplets are essential for the development of preimplantation embryos (seeds) and for preventing lipotoxicity [54]. For the endometrium (soil), a report of lipid droplet accumulation during the ESC decidual process [11] was consistent with our results. In addition, the knockdown of ACSL4 was able to reduce the level of lipid droplet accumulation, suggesting that lipid droplet synthesis during the ESC decidual process is regulated by ACSL4. Interestingly, although decidualization stimulates lipid droplet accumulation in ESCs, it is not impaired by the pharmacological and genetic inhibition of lipid droplet synthesis. This suggests that the accumulation of lipid droplets is not necessary for the decidua and that the storage of lipid droplets during the decidual process may have other functions.

The process of embryo invasion into decidual cells is strictly regulated by the endometrial microenvironment [55]. Lipid metabolism of the uterus affects the development of the embryo [5], and endometrial cells are considered to be an important source of nutrients for the embryo [56–58]. Since the decidual cells surrounding the embryo are embedded in the endometrium, lipid droplets stored in the decidua may provide energy/nutrients directly to the embryo. Evidence suggests that lipids are an important nutrient source for embryonic development [59]. The accumulation of lipid droplets does not affect decidualization, suggesting that the decidua may serve as a nutrient storage site for embryos. Our previous studies have shown that glucose metabolism in endometrial cells regulates endometrial receptivity and embryo implantation [2,25]; one characteristic of the decidua is glucose uptake increase and energy production [58]. Except for glucose, FAs are an important source of energy for cells [60]. Here, we also observed that the expression of CPT1A and CPT2, key enzymes for FA β-oxidation, was increased during the decidual process and that the knockdown of ACSL4 decreased their expression. These results indicate that the FAs activated by ACSL4 flow to lipid droplet synthesis and β-oxidation, respectively. Pharmacological and genetic inhibition of FA β-oxidation was able to impair the ESC decidual process, suggesting that FA β-oxidation is required for decidualization and that ACSL4 may regulate decidualization through a β-oxidation pathway.

Studies have shown that liver-specific acyl-CoA oxidase 1 knockout (the enzyme in the first step that catalyzes peroxisomal β-oxidation) protects mice from hepatic steatosis caused by starvation or a high-fat diet by inducing autophagy degradation of lipid droplets [61]. Inhibition of medium-chain acyl-CoA dehydrogenase (an enzyme that catalyzes the first step of mitochondrial FA β-oxidation) promotes hepatocellular carcinoma cell motility and increases levels of TAG, phospholipids, and cellular lipid droplets [62]. Although no direct evidence exists on the specific mechanism of the mutual regulation between β-oxidation and lipid droplet accumulation, the evidence also fully indicates crosstalk between β-oxidation and lipid droplet accumulation. The effect of β-oxidation on lipid droplet synthesis may not be the same (or even the opposite) under different conditions. During the ESC decidual process, we observed the accumulation of lipid droplets and the enhancement of β-oxidation, respectively; whether the two interact with each other has aroused our interest. We found no effect on β-oxidation after the synthesis of the pharmacological and genetic inhibition of lipid droplets. However, the pharmacological and genetic inhibition of β-oxidation increased lipid droplet accumulation. These results indirectly validate our finding that neither the inhibition nor increase (induced by inhibition of β-oxidation) in lipid droplet accumulation affects decidualization (decidualization is not affected whether lipid droplet accumulation increases or inhibits). Since ACSL4 regulates lipid droplet accumulation and FA β-oxidation, respectively, and β-oxidation is critical for the ESC decidual process, we hypothesized that ACSL4 might affect decidualization through a β-oxidation pathway. Our subsequent experiments adequately verified this speculation because activation of β-oxidation was able to reverse the decidualization damage induced by ACSL4 knockdown.

Since ACSL4 regulates the decidual process through the β-oxidation pathway, the question arises as to what the mechanism is behind blocking FA β-oxidation that leads to damaged decidualization. The products of FA β-oxidation include flavin adenine dinucleotide ($FADH_2$), nicotinamide adenine dinucleotide (NADH), and acetyl-CoA. The latter enters the TCA cycle to produce energy. Evidence suggests that decidua increases glucose uptake and the expression of glucose transporter type 1 [63,64]. Our previous findings also indicate that glucose metabolism is crucial for embryo implantation [2,25], suggesting that an adequate energy supply may be a prerequisite for maintaining the decidua. In addition, the importance of other products of β-oxidation ($FADH_2$, NADH, and intermediate metabolic lipids) to the decidua cannot be ruled out. Moreover, studies have shown that downregulation of CPT1A activates the phosphatidylinositol 3-kinase (PI3K)/protein kinase B (PKB/AKT) pathway [29], which inhibits decidualization [65,66]. Inhibition of CPT1A stimulates phosphorylation of the FoxO transcription factor [67], while the phosphorylation of FoxO1 promotes self-degradation and damages decidualization [68]. These studies suggest that inhibition of decidualization by β-oxidation may also be related to several signaling pathways and proteins which are mediated by CPT1A downregulation. If ACSL4-mediated lipid catabolism has a similar effect to glucose metabolism, what is the difference between glucose metabolism and lipid metabolism in triggering decidualization? That would be a question worth thinking about. In addition, the identification of specific FAs activated by ACSL4 would be a worthwhile and in-depth endeavor.

Overall, we found that ACSL4 was highly expressed in the endometrium during implantation, and lipid anabolism and catabolism were enhanced during ESC decidualization. Knockdown of ACSL4 inhibits FA β-oxidation and lipid droplet accumulation and impairs decidualization. Interestingly, pharmacological and genetic inhibition of lipid droplet synthesis did not affect FA β-oxidation and decidualization, while the pharmacological and genetic inhibition of FA β-oxidation increased lipid droplet accumulation and inhibited decidualization. The decidualization damage caused by ACSL4 knockdown could be reversed by activating β-oxidation. These results suggest that ACSL4-activated fatty acyl-CoA may activate decidualization through the β-oxidation

pathway. ACSL4 may be a target for the treatment of decidua abnormalities and implantation failure, and its study provides new insights into the effects of lipid metabolism on embryo implantation.

FUNDING

This study was supported by the National Natural Science Foundation of China (82301908, 31400687), the Liaoning Revitalization Talents Program (XLYC2211013), the Research Project of Education Department of Liaoning Province (LJKQZ20222417), and the Doctoral Research Initiation Fund Project of Liaoning Province (2023-BSBA-094), the Scientific Research Fund of Dalian Ruining Biotechnology Co., Ltd. (505626).

CREDIT AUTHORSHIP CONTRIBUTION STATEMENT

Hongshuo Zhang: Writing — original draft, Visualization, Project administration, Funding acquisition, Conceptualization. **Qianyi Sun:** Writing — review & editing, Visualization, Software, Investigation, Formal analysis, Data curation. **Haojie Dong:** Visualization, Software, Formal analysis, Data curation. **Zeen Jin:** Formal analysis, Data curation. **Mengyue Li:** Formal analysis, Data curation. **Shanyuan Jin:** Formal analysis, Data curation. **Xiaolan Zeng:** Formal analysis, Data curation. **Jianhui Fan:** Writing — review & editing, Resources, Methodology. **Ying Kong:** Writing — review & editing, Project administration, Funding acquisition, Conceptualization.

DECLARATION OF COMPETING INTEREST

The authors declare that there are no conflicts of interest.

DATA AVAILABILITY

No data was used for the research described in the article.

APPENDIX A. SUPPLEMENTARY DATA

Supplementary data to this article can be found online at https://doi.org/10.1016/j.molmet.2024.101953.

REFERENCES

[1] Ng SW, Norwitz GA, Pavlicev M, Tilburgs T, Simón C, Norwitz ER. Endometrial decidualization: the primary driver of pregnancy health. Int J Mol Sci 2020;21(11).

[2] Zhang H, Qi J, Wang Y, Sun J, Li Z, Sui L, et al. Progesterone regulates glucose metabolism through glucose transporter 1 to promote endometrial receptivity. Front Physiol 2020;11:543148.

[3] Liu Y, Yao Y, Sun H, Zhao J, Li H, Wang S, et al. Lipid metabolism-related genes as biomarkers and therapeutic targets reveal endometrial receptivity and immune microenvironment in women with reproductive dysfunction. J Assist Reprod Genet 2022;39(9):2179—90.

[4] Matorras R, Martinez-Arranz I, Arretxe E, Iruarrizaga-Lejarreta M, Corral B, Ibañez-Perez J, et al. The lipidome of endometrial fluid differs between implantative and non-implantative IVF cycles. J Assist Reprod Genet 2020;37(2):385—94.

[5] Ye Q, Zeng X, Cai S, Qiao S, Zeng X. Mechanisms of lipid metabolism in uterine receptivity and embryo development. Trends Endocrinol Metab 2021;32(12):1015—30.

[6] Gonzalez MB, Robker RL, Rose RD. Obesity and oocyte quality: significant implications for ART and emerging mechanistic insights. Biol Reprod 2022;106(2):338—50.

[7] Demiral İ, Doğan M, Baştu E, Buyru F. Genomic, proteomic and lipidomic evaluation of endometrial receptivity. Turk J Obstet Gynecol 2015;12(4):237—43.

[8] Yang T, Zhao J, Liu F, Li Y. Lipid metabolism and endometrial receptivity. Hum Reprod Update 2022;28(6):858—89.

[9] Fattahi A, Darabi M, Farzadi L, Salmassi A, Latifi Z, Mehdizadeh A, et al. Effects of dietary omega-3 and -6 supplementations on phospholipid fatty acid composition in mice uterus during window of pre-implantation. Theriogenology 2018;108:97—102.

[10] Rhee JS, Saben JL, Mayer AL, Schulte MB, Asghar Z, Stephens C, et al. Diet-induced obesity impairs endometrial stromal cell decidualization: a potential role for impaired autophagy. Hum Reprod 2016;31(6):1315—26.

[11] Tamura I, Takagi H, Doi-Tanaka Y, Shirafuta Y, Mihara Y, Shinagawa M, et al. Wilms tumor 1 regulates lipid accumulation in human endometrial stromal cells during decidualization. J Biol Chem 2020;295(14):4673—83.

[12] Soupene E, Kuypers FA. Mammalian long-chain acyl-CoA synthetases. Exp Biol Med (Maywood) 2008;233(5):507—21.

[13] Chen WC, Wang CY, Hung YH, Weng TY, Yen MC, Lai MD. Systematic analysis of gene expression alterations and clinical outcomes for long-chain acyl-coenzyme A synthetase family in cancer. PLoS One 2016;11(5):e0155660.

[14] Li LO, Grevengoed TJ, Paul DS, Ilkayeva O, Koves TR, Pascual F, et al. Compartmentalized acyl-CoA metabolism in skeletal muscle regulates systemic glucose homeostasis. Diabetes 2015;64(1):23—35.

[15] Fernandez RF, Kim SQ, Zhao Y, Foguth RM, Weera MM, Counihan JL, et al. Acyl-CoA synthetase 6 enriches the neuroprotective omega-3 fatty acid DHA in the brain. Proc Natl Acad Sci U S A 2018;115(49):12525—30.

[16] Klaus C, Schneider U, Hedberg C, Schütz AK, Bernhagen J, Waldmann H, et al. Modulating effects of acyl-CoA synthetase 5-derived mitochondrial Wnt2B palmitoylation on intestinal Wnt activity. World J Gastroenterol 2014;20(40):14855—64.

[17] Kang MJ, Fujino T, Sasano H, Minekura H, Yabuki N, Nagura H, et al. A novel arachidonate-preferring acyl-CoA synthetase is present in steroidogenic cells of the rat adrenal, ovary, and testis. Proc Natl Acad Sci U S A 1997;94(7):2880—4.

[18] Wu X, Li Y, Wang J, Wen X, Marcus MT, Daniels G, et al. Long chain fatty acyl-CoA synthetase 4 is a biomarker for and mediator of hormone resistance in human breast cancer. PLoS One 2013;8(10):e77060.

[19] Cao Y, Dave KB, Doan TP, Prescott SM. Fatty acid CoA ligase 4 is up-regulated in colon adenocarcinoma. Cancer Res 2001;61(23):8429—34.

[20] Sung YK, Hwang SY, Park MK, Bae HI, Kim WH, Kim JC, et al. Fatty acid-CoA ligase 4 is overexpressed in human hepatocellular carcinoma. Cancer Sci 2003;94(5):421—4.

[21] Chen J, Ding C, Chen Y, Hu W, Yu C, Peng C, et al. ACSL4 reprograms fatty acid metabolism in hepatocellular carcinoma via c-Myc/SREBP1 pathway. Cancer Lett 2021;502:154—65.

[22] Kuwata H, Hara S. Role of acyl-CoA synthetase ACSL4 in arachidonic acid metabolism. Prostaglandins Other Lipid Mediat 2019;144:106363.

[23] Huang J, Xue M, Zhang J, Yu H, Gu Y, Du M, et al. Protective role of GPR120 in the maintenance of pregnancy by promoting decidualization via regulation of glucose metabolism. EBioMedicine 2019;39:540—51.

[24] Zeng S, Wu F, Chen M, Li Y, You M, Zhang Y, et al. Inhibition of fatty acid translocase (FAT/CD36) palmitoylation enhances hepatic fatty acid β-oxidation by increasing its localization to mitochondria and interaction with long-chain acyl-CoA synthetase 1. Antioxid Redox Signal 2022;36(16—18):1081—100. https://doi.org/10.1089/ars.2021.0157.

[25] Zhang H, Qi J, Pei J, Zhang M, Shang Y, Li Z, et al. O-GlcNAc modification mediates aquaporin 3 to coordinate endometrial cell glycolysis and affects embryo implantation. J Adv Res 2022;37:119—31.

[26] Peñuelas-Haro I, Espinosa-Sotelo R, Crosas-Molist E, Herranz-Itúrbide M, Caballero-Díaz D, Alay A, et al. The NADPH oxidase NOX4 regulates redox and metabolic homeostasis preventing HCC progression. Hepatology 2023;78(2):416–33. https://doi.org/10.1002/hep.32702.

[27] Chen YQ, Kuo MS, Li S, Bui HH, Peake DA, Sanders PE, et al. AGPAT6 is a novel microsomal glycerol-3-phosphate acyltransferase. J Biol Chem 2008;283(15):10048–57.

[28] Jiang N, Xie B, Xiao W, Fan M, Xu S, Duan Y, et al. Fatty acid oxidation fuels glioblastoma radioresistance with CD47-mediated immune evasion. Nat Commun 2022;13(1):1511.

[29] Chen M, Chao B, Xu J, Liu Z, Tao Y, He J, et al. CPT1A modulates PI3K/Akt/mTOR pathway to promote preeclampsia. Placenta 2023;133:23–31.

[30] Nisticò C, Pagliari F, Chiarella E, Fernandes Guerreiro J, Marafioti MG, Aversa I, et al. Lipid droplet biosynthesis impairment through DGAT2 inhibition sensitizes MCF7 breast cancer cells to radiation. Int J Mol Sci 2021;22(18).

[31] Bhatt-Wessel B, Jordan TW, Miller JH, Peng L. Role of DGAT enzymes in triacylglycerol metabolism. Arch Biochem Biophys 2018;655:1–11. https://doi.org/10.1016/j.abb.2018.08.001.

[32] Chitraju C, Mejhert N, Haas JT, Diaz-Ramirez LG, Grueter CA, Imbriglio JE, et al. Triglyceride synthesis by DGAT1 protects adipocytes from lipid-induced ER stress during lipolysis. Cell Metab 2017;26(2):407–418.e3. https://doi.org/10.1016/j.cmet.2017.07.012.

[33] Selvaraj R, Zehnder SV, Watts R, Lian J, Das C, Nelson R, et al. Preferential lipolysis of DGAT1 over DGAT2 generated triacylglycerol in Huh7 hepatocytes. Biochim Biophys Acta Mol Cell Biol Lipids 2023;1868(10):159376. https://doi.org/10.1016/j.bbalip.2023.159376.

[34] Thupari JN, Landree LE, Ronnett GV, Kuhajda FP. C75 increases peripheral energy utilization and fatty acid oxidation in diet-induced obesity. Proc Natl Acad Sci U S A 2002;99(14):9498–502.

[35] Impheng H, Richert L, Pekthong D, Scholfield CN, Pongcharoen S, Pungpetchara I, et al. [6]-Gingerol inhibits de novo fatty acid synthesis and carnitine palmitoyltransferase-1 activity which triggers apoptosis in HepG2. Am J Cancer Res 2015;5(4):1319–36.

[36] Gomez-Martinez I, Bliton RJ, Breau KA, Czerwinski MJ, Williamson IA, Wen J, et al. A planar culture model of human absorptive enterocytes reveals metformin increases fatty acid oxidation and export. Cell Mol Gastroenterol Hepatol 2022;14(2):409–34.

[37] Bentebibel A, Sebastián D, Herrero L, López-Viñas E, Serra D, Asins G, et al. Novel effect of C75 on carnitine palmitoyltransferase I activity and palmitate oxidation. Biochemistry 2006;45(14):4339–50.

[38] Elis S, Desmarchais A, Maillard V, Uzbekova S, Monget P, Dupont J. Cell proliferation and progesterone synthesis depend on lipid metabolism in bovine granulosa cells. Theriogenology 2015;83(5):840–53.

[39] Yang X, Chen J, Lu Z, Huang S, Zhang S, Cai J, et al. Enterovirus A71 utilizes host cell lipid β-oxidation to promote its replication. Front Microbiol 2022;13:961942.

[40] Dai J, Liang K, Zhao S, Jia W, Liu Y, Wu H, et al. Chemoproteomics reveals baicalin activates hepatic CPT1 to ameliorate diet-induced obesity and hepatic steatosis. Proc Natl Acad Sci U S A 2018;115(26):E5896–905.

[41] Hosseini M, Poljak A, Braidy N, Crawford J, Sachdev P. Blood fatty acids in Alzheimer's disease and mild cognitive impairment: a meta-analysis and systematic review. Ageing Res Rev 2020;60:101043.

[42] Hou J, Jiang C, Wen X, Li C, Xiong S, Yue T, et al. ACSL4 as a potential target and biomarker for anticancer: from molecular mechanisms to clinical therapeutics. Front Pharmacol 2022;13:949863.

[43] Küch EM, Vellaramkalayil R, Zhang I, Lehnen D, Brügger B, Sreemmel W, et al. Differentially localized acyl-CoA synthetase 4 isoenzymes mediate the metabolic channeling of fatty acids towards phosphatidylinositol. Biochim Biophys Acta 2014;1841(2):227–39.

[44] Tang Y, Zhou J, Hooi SC, Jiang YM, Lu GD. Fatty acid activation in carcinogenesis and cancer development: essential roles of long-chain acyl-CoA synthetases. Oncol Lett 2018;16(2):1390–6.

[45] Rossi Sebastiano M, Konstantinidou G. Targeting long chain acyl-CoA synthetases for cancer therapy. Int J Mol Sci 2019;20(15).

[46] Wang XJ, Dyson MT, Jo Y, Eubank DW, Stocco DM. Involvement of 5-lipoxygenase metabolites of arachidonic acid in cyclic AMP-stimulated steroidogenesis and steroidogenic acute regulatory protein gene expression. J Steroid Biochem Mol Biol 2003;85(2–5):159–66.

[47] Kagan VE, Mao G, Qu F, Angeli JP, Doll S, Croix CS, et al. Oxidized arachidonic and adrenic PEs navigate cells to ferroptosis. Nat Chem Biol 2017;13(1):81–90.

[48] Shui S, Zhao Z, Wang H, Conrad M, Liu G. Non-enzymatic lipid peroxidation initiated by photodynamic therapy drives a distinct ferroptosis-like cell death pathway. Redox Biol 2021;45:102056.

[49] Cho YY, Kang MJ, Sone H, Suzuki T, Abe M, Igarashi M, et al. Abnormal uterus with polycysts, accumulation of uterine prostaglandins, and reduced fertility in mice heterozygous for acyl-CoA synthetase 4 deficiency. Biochem Biophys Res Commun 2001;284(4):993–7.

[50] Hu S, Sun Z, Li B, Zhao H, Wang Y, Yao G, et al. iTRAQ-based proteomic analysis unveils ACSL4 as a novel potential regulator of human endometrial receptivity. Endocrinology 2023;164(3).

[51] Waclawik A, Kaczmarek MM, Blitek A, Kaczynski P, Ziecik AJ. Embryo-maternal dialogue during pregnancy establishment and implantation in the pig. Mol Reprod Dev 2017;84(9):842–55.

[52] Almada M, Amaral C, Diniz-da-Costa M, Correia-da-Silva G, Teixeira NA, Fonseca BM. The endocannabinoid anandamide impairs in vitro decidualization of human cells. Reproduction 2016;152(4):351–61.

[53] Vasquez YM, DeMayo FJ. Role of nuclear receptors in blastocyst implantation. Semin Cell Dev Biol 2013;24(10–12):724–35.

[54] Aizawa R, Ibayashi M, Tatsumi T, Yamamoto A, Kokubo T, Miyasaka N, et al. Synthesis and maintenance of lipid droplets are essential for mouse preimplantation embryonic development. Development 2019;146(22).

[55] Gellersen B, Brosens JJ. Cyclic decidualization of the human endometrium in reproductive health and failure. Endocr Rev 2014;35(6):851–905.

[56] Burton GJ, Hempstock J, Jauniaux E. Nutrition of the human fetus during the first trimester–a review. Placenta 2001;22(Suppl A):S70–7.

[57] Burton GJ, Watson AL, Hempstock J, Skepper JN, Jauniaux E. Uterine glands provide histiotrophic nutrition for the human fetus during the first trimester of pregnancy. J Clin Endocrinol Metab 2002;87(6):2954–9.

[58] Tamura I, Shiroshita A, Fujimura T, Tanaka-Doi Y, Shirafuta Y, Taketani T, et al. Glucose and lipid metabolisms in human endometrial stromal cells during decidualization. Endocr J 2023;70(5):465–72.

[59] Tatsumi T, Takayama K, Ishii S, Yamamoto A, Hara T, Minami N, et al. Forced lipophagy reveals that lipid droplets are required for early embryonic development in mouse. Development 2018;145(4).

[60] Citrinovitz A, Hauke J, Jauckus J, Langhans CD, Schwarz K, Zorn M, et al. Glucose and fatty acids catabolism during in vitro decidualization of human endometrial stromal cells. J Assist Reprod Genet 2022;39(12):2689–97.

[61] He A, Chen X, Tan M, Chen Y, Lu D, Zhang X, et al. Acetyl-CoA derived from hepatic peroxisomal β-oxidation inhibits autophagy and promotes steatosis via mTORC1 activation. Mol Cell 2020;79(1):30–42.e4.

[62] Ma A, Yeung C, Tey SK, Mao X, Wong S, Ng TH, et al. Suppression of ACADM-mediated fatty acid oxidation promotes hepatocellular carcinoma via aberrant CAV1/SREBP1 signaling. Cancer Res 2021;81(13):3679–92.

[63] Frolova A, Flessner L, Chi M, Kim ST, Foyouzi-Yousefi N, Moley KH. Facilitative glucose transporter type 1 is differentially regulated by progesterone and estrogen in murine and human endometrial stromal cells. Endocrinology 2009;150(3):1512–20.

[64] Frolova AI, Moley KH. Quantitative analysis of glucose transporter mRNAs in endometrial stromal cells reveals critical role of GLUT1 in uterine receptivity. Endocrinology 2011;152(5):2123–8.
[65] Fabi F, Grenier K, Parent S, Adam P, Tardif L, Leblanc V, et al. Regulation of the PI3K/Akt pathway during decidualization of endometrial stromal cells. PLoS One 2017;12(5):e0177387.
[66] Wei M, Gao Y, Lu B, Jiao Y, Liu X, Cui B, et al. FKBP51 regulates decidualization through Ser473 dephosphorylation of AKT. Reproduction 2018;155(3):283–95.
[67] Shao H, Mohamed EM, Xu GG, Waters M, Jing K, Ma Y, et al. Carnitine palmitoyltransferase 1A functions to repress FoxO transcription factors to allow cell cycle progression in ovarian cancer. Oncotarget 2016;7(4):3832–46.
[68] Peng Y, Liu X, Jin Z, Liu H, Xu C. Scribble downregulation in adenomyosis compromises endometrial stromal decidualization by decreasing FOXO1 expression. Hum Reprod 2021;37(1):93–108.

